Talanta 99 (2012) 375–379

Contents lists available at SciVerse ScienceDirect

Talanta

journal homepage: www.elsevier.com/locate/talanta

MicroRNA detection using lateral flow nucleic acid strips with gold nanoparticles

Shao-Yi Hou [a,b,*], Yi-Ling Hsiao [a], Ming-Shu Lin [a], Chun-Che Yen [c], Chi-Sheng Chang [c]

[a] Institute of Biotechnology, National Taipei University of Technology, 1, Sec. 3, Chung-Hsiao E. Road, Taipei 106, Taiwan
[b] Department of Chemical Engineering, National Taipei University of Technology, 1, Sec. 3, Chung-Hsiao E. Road, Taipei 106, Taiwan
[c] Center for Measurement Standards, Industrial Technology Research Institute, 195, Sec. 4, Chung Hsing Road, Chutung, Hsinchu 31040, Taiwan

ARTICLE INFO

Article history:
Received 15 March 2012
Received in revised form
31 May 2012
Accepted 31 May 2012
Available online 17 June 2012

Keywords:
MicroRNA detection
Lateral flow nucleic acid strips
Gold nanoparticles
Mung-bean nuclease
Single-strand-specific nuclease

ABSTRACT

In this study, the tested microRNA and the detection probe perfectly match with the capture probe instead of the traditional sandwich methods in which the tested oligonucleotide matches with the detection and capture probes. To avoid non-specific signals, mung-bean nuclease, a single-strand-specific nuclease, catalyzes the degradation of the capture probe if there is no tested miRNA in the samples. The gold nanoparticles conjugate the thiol-DNA as the detection probe and the biotin-single strand DNA serves as the capture probe. The avidin–biotin–Au-sample complex is captured by the anti-avidin antibody immobilized on a flow strip. The detection and quantification of the gold nanoparticle signal indicate the existence and quantity of the target miRNA. One fmol and five amol of the synthetic microRNA were detected without and with the silver enhancement, respectively. This highly sensitive and specific assay takes about 70 min after the RNA purification and preparation. It is simple, convenient, fast, and suitable for point-of-care.

1. Introduction

MicroRNA (miRNA, 21–25 nts) and small interfering RNA (siRNA, 21–25 nts) belong to a group of non-protein-coding and regulatory molecules, called small RNAs, including small nuclear RNA (106–185 nts), small nucleolar RNA (60–300 nts), bacterial small RNA (50–250 nts) and others [1]. Recently, siRNA and miRNA have been demonstrated to play roles in biological processes ranging from developmental regulation, stress responses, cell differentiation, and cardiogenesis, to epigenetic inheritance [2,3]. Hence, a simple, fast, and sensitive miRNA or siRNA quantification method will help disease detection, therapy validation and point-of-care.

One of the challenges for miRNA or siRNA detection is that the nucleic acid sandwich methods, an oligonucleotide capture probe on a membrane or glass and an oligonucleotide detection probe with a signal, may not work well. The small sizes of these two small RNAs limit the lengths of the two probes. Hence, the annealing temperatures of the probes may be below room temperature which causes the hybridization between the probes and the small RNAs to be difficult or even impossible. Furthermore, with small hybridization probes, the stringency of the hybridization decreases and the risk of cross-hybridization significantly increases. If a method is not selective enough, the mismatch in one or several bases may still produce a signal, thus giving a false positive reading [4].

The current gold standard method for miRNA validation is northern blotting [5]. It uses only an oligonucleotide probe, as the detection probe, because the membrane transfer immobilizes the RNA samples without a capture probe, and the gel electrophoresis separating different length RNAs provides another characteristic to identify the tested miRNA in northern blotting. However, even with improvements in the sensitivity provided by the digoxigenin labeled RNA probes [6], a splinted ligation strategy [7], enhanced cross-linking of the RNA to membranes [8], or locked nucleic acid-modified oligonucleotides [9], northern blotting still takes days to semi-quantify the miRNA or siRNA [10]. Many other assays for detecting miRNAs have been developed including a pyrophosphate-based method [11], an electrochemical approach [12], a PCR-based method [13], peptide nucleic acid-based assays [14], an ELISA-based assay [15], nanoparticle-based assays [5], bead-based assays [16], an Invader assay [17], and microarray-based approaches [18]. Many of these methods require equipments and others involve amplification reactions. This impedes these methods from applying for point-of-care.

Gold nanoparticles (AuNP) have been used in different bioassay readout techniques over the past two decades, because of their easily controllable size distribution, long-term stability, and good biocompatibility with proteins, DNA, and RNA [19]. Recently, one of their applications was the emerging lateral flow nucleic acid (LFNA) test strips [20,21], adopted from the well-developed immunochromatography strip technology [22,23]. Glynou et al. reported an LFNA strip, called the dry-reagent strip biosensor, based on an oligonucleotide detection probe labeled with AuNP for visual detection of

* Corresponding author at: National Taipei University of Technology Department of Chemical Engineering 1, Sec. 3, Chung-Hsiao E. Road, Taipei 106, Taiwan.
E-mail addresses: ericklin710516@gmail.com, f10955@ntut.edu.tw (S.-Y. Hou).

0039-9140/$ - see front matter © 2012 Elsevier B.V. All rights reserved.
http://dx.doi.org/10.1016/j.talanta.2012.05.067

the DNA [24]. The test strips have been used for the visual detection of virus or bacterial infection [23], point-mutation [25], and genetically modified organisms [26]. All of them used the traditional nucleic acid sandwich methods which cannot work well for miRNA detection. Colloid gold was originally used as tracers in the electron microscopic studies of cellular samples [27]. The signal could be intensified by the reaction that precipitates silver on the nanogold and the labels were visible by optical microscopy [27]. Recently, a set of silver enhancement reagents was used to amplify the colloidal gold signal in the assays [19,28].

The single-strand-specific nucleases endonucleolytically catalyze the degradation of single-stranded DNA (ssDNA) and RNA. These nucleases prefer ssDNA over the double-stranded DNA or DNA–RNA complex by 30,000-fold [29,30]. They even cleave at a single-nucleotide mismatch when the two nucleic acid strands are not a perfect match [31]. The zinc ion is the cofactor for the single-strand-specific nucleases; hence, ethylenediaminetetraacetic acid (EDTA) is used to inhibit the enzyme's activity [29].

In this study, the tested miRNA and the detection probe perfectly match with the capture probe (Fig. 1) instead of the traditional sandwich methods in which the tested oligonucleotide match with the detection and capture probes. Mung-bean nuclease, a single-strand-specific nuclease, catalyzes the degradation of the capture probe if there is no tested miRNA in the samples. The proposed method is simple, convenient, fast, and suitable for point-of-care.

2. Experimental section

2.1. Reagents

All the used oligonucleotides are listed in Table 1. The probes and the synthetic miRNAs were purchased from Scientific Biotech (Taipei, Taiwan) and MDBio (Taipei, Taiwan), respectively. The gold nanoparticles (Nano Gold-40) were purchased from Taiwan Advanced Nanotech, Inc. (Taoyuan, Taiwan). The sizes of nanogold were between 25 and 35 nm. Mung bean nuclease (cat. no. M4311) and its reaction buffer (cat. no. M4311) were both purchased from Promega (Madison, WI, USA). The silver enhancer kit (cat. no. SE-100), the antibody against biotin (cat. no. B7653), 1-undecanethiol (cat. no. 510467), and bovine serum albumin (BSA; cat. no. A9647) were purchased from Sigma (St. Louis, MO). The nitrocellulose membranes were purchased from Bio-Rad (Hercules, CA). The RNase inhibitor (cat. no. EO0382) was purchased from Fermentas (Burlington, Ontario). DEPC-treated water was used for all the buffers to prevent RNA degradation by RNAse.

2.2. Preparation of oligonucleotide-modified gold nanoparticles

The detection probe–gold nanoparticle conjugates were prepared as previously described [31]. Briefly, 10 μl of the 100 μM thiol-modified detection probe was added to 500 μl of a gold nanoparticle solution. After 16 h, the colloid solution was added to a 10 mM phosphate buffer (PB: NaH_2PO_4/Na_2HPO_4) solution. The colloids were gradually added to 0.3 M NaCl by the dropwise addition of the 2 M NaCl solution. After centrifugation, the precipitate was washed, recentrifuged, and redispersed in a 0.3 M NaCl and 10 mM PB (PBS) solution. After being washed twice, the colloid was resuspended in a 0.01% azide PBS solution and then stored at 4 °C. Before the assay, 1-undecanethiol (UDT) was used to block the remaining surface of the nanogold. The different amounts of UDT were added to the solution of the detection probe–gold nanoparticle conjugates. After 1 h, the solution was centrifuged and the precipitate was resuspended in PBS solution.

2.3. Preparation of the lateral flow strip

The anti-avidin antibody diluted to 0.5 mg/mL with PBS was used as the test line capture reagent and dispensed by the BioJet Quanti3000™ dispenser onto a nitrocellulose membrane as the test line of the LFNA test strips. After soaking in 5% BSA for 30 min at room temperature to block the rest of the nitrocellulose and dried in an incubator at 30 °C for 30 min, the membranes were stored in bags. Before the assay, the membrane was stuck to an absorption pad.

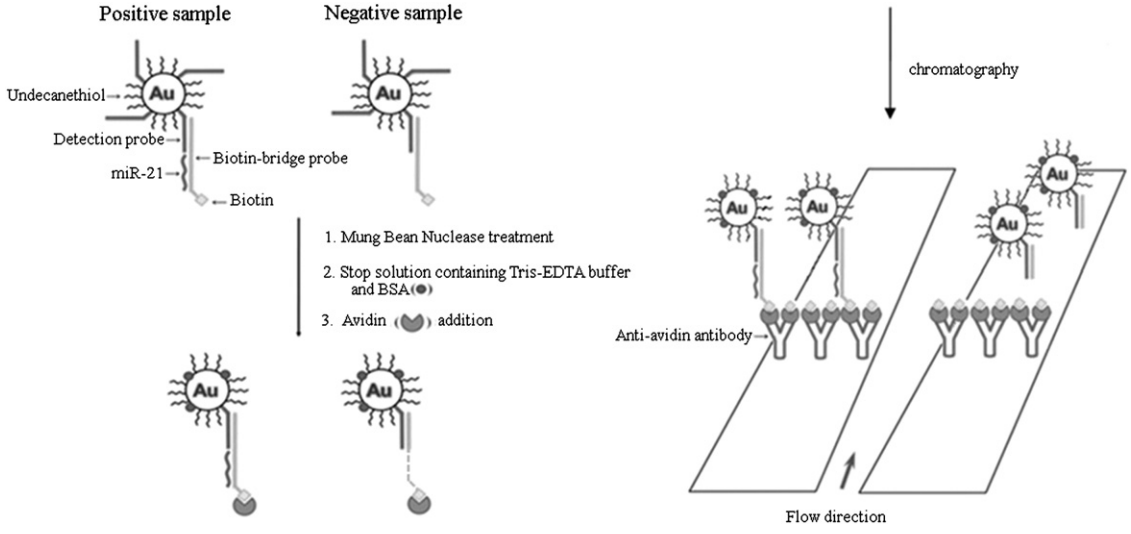

Fig. 1. Schematic description of the proposed method.

Table 1
Oligonucleotides in this study.

Detection probe	5′–HS-(CH2)12-AAAAAAAAAATTAACCACAACACCTTCCTCCCCG–3′
Biotin-bridge probe	5′–Biotin-TCAACATCAGTCTGATAAGCTACGGGGAGGAAGGTGTTGTGGTTAATTTTTTTTTT–3′
Synthetic miRNA-21	5′–UAGCUUAUCAGACUGAUGUUGA–3′

2.4. Assay procedure

Fig. 1 is a schematic description of the proposed assay used in this study. In a typical test, 50 μL of detection probe–AuNP conjugates (0.355 nM) were mixed with 100 fmol of the biotin-bridge probe and different amounts of synthetic mi-RNA 21 for 30 min. After hybridization, the mix was treated with 1 unit of mung bean nuclease at 30 °C in the reaction buffer containing 30 mM of sodium acetate and 1 mM of zinc chloride. After a 15 min treatment, 50 μL of the stop solution containing TE buffer (pH 8), 5% BSA, and 16 pmol of avidin was added for 10 min. The end without the absorption pad of the test strip was soaked in the above mentioned mix for about 10 min. The total assay time was about 70 min. In order to detect very low levels of the tested miRNA, silver enhancement reagents were used to intensify the signal of the gold nanoparticles. The above tested membranes were soaked in silver enhancer solutions for 15 min at room temperature.

2.5. Quantitative analysis

The relative amount of each band was scored using Quantity One (Bio-Rad) [19]. One μL of methyl red (0.5 μg) was used as the external standard. The intensity volumes of the methyl red (Im), the sample (I), and the empty area (I0), the regions containing the same areas as the bands or the methyl red dots just next to the bands or the methyl red dots, were measured. The relative intensity is defined as (I−I0)/(Im−I0). Each point or column in Figs. 2B, 3B, and 5 represents the mean of the measurements. The 95% confidence interval for each mean is between the error bars (Figs. 2B, 3B, and 5).

3. Results and discussion

3.1. Assay design

A schematic representation of the design of the proposed method is shown in Fig. 1. The tested miRNA and the detection probe perfectly match with the capture probe, indicated as the biotin-bridge probe in Fig. 1. The predicted melting temperature of miRNA-21, the model miRNA in this study, is 47 °C based on the calculation using Vector NTI Advance, a computer program. Hence, it is able to bind the capture probe at room temperature. However, based on the Vector NTI Advance, the predicted melting temperatures of the first 11nt and the last 11nt of miRNA-21 are 11 °C and 15 °C, respectively. Using the traditional sandwich method, the hybridization between the two probes and miRNA-21 is impossible at room temperature if the two probes are complement with the first 11nt and the last 11nt of miRNA-21. Mung-bean nuclease is used to degrade the nonbinding capture probe and the nonbinding detection probe. The stop solution contains Tris–EDTA buffer to chelate the zinc ions, the cofactor for mung-bean nuclease, and BSA to block the naked area of the surface of the nanogold formed after the single-strand-specific nuclease degrades the nonbinding detection probe. After avidin addition and flow through the LFNA strips, red bands were observed on the LFNA strips due to the accumulation of AuNP on the test zone containing the anti-avidin antibody.

3.2. Working range and detection limit without silver enhancement

The experimental procedures are described in the Experimental Section. A series of dilutions of the synthetic microRNA-21 (miR-21) was prepared in PBS. In Fig. 2A, the intensity is proportional to the miR-21 concentration in the range of 100 fmol to 10 fmol when the concentration of the biotin-bridge probe is 100 fmol. The images for the 1 fmol and 5 fmol were faint but visible, and no band was observed in the negative control (Fig. 2A). The densitometry analysis for each band was executed using Quantity One. The definition of the relative intensity is stated in the experimental section. Fig. 2B shows the standard curve for the miR-21 generated by this method. The correlation coefficient of the data for the linearized portion of the curve between 100 fmol and 10 fmol of the miR-21 was 0.944. The equation for the linear fit is relative intensity = 0.128 + 0.0022 miR-21(fmol). The 95% confidence interval for each mean is between the error bars (Fig. 2B). Some of them are significant. Hence, a standard curve should be generated for each set of samples assayed by this method.

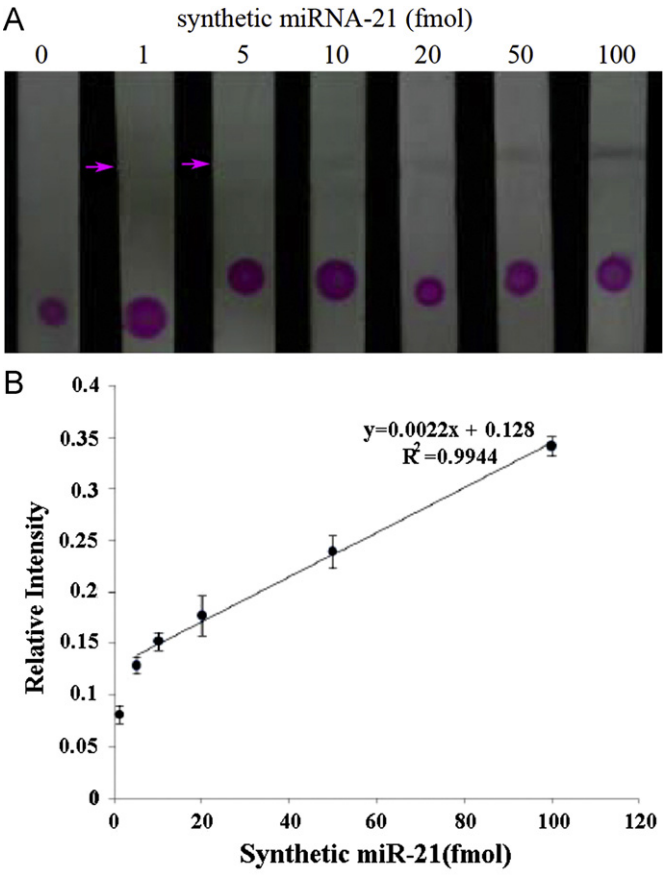

Fig. 2. Detection of miRNA-21 without silver enhancement. (A) Red band images for different levels of the miRNA-21. (B) Detection curve for miRNA-21. Each point represents the mean of six measurements from six separate experiments. The 95% confidence interval for each mean is between the error bars. The concentration of UDT, the blocking agent in this study, is 2.23 nM. The hybridization and mung-bean reaction times are 30 and 15 min, respectively. The volume of DEPC-treated water containing tested miRNA is 100 μl. (For interpretation of the references to color in this figure legend, the reader is referred to the web version of this article.)

3.3. Working range and detection limit with silver enhancement

In order to increase the sensitivity of this detection method, the silver enhancement method was used. The procedures are described in the Experimental Section. Fig. 3A shows the detection limit to be as low as 5 amol. In the absence of the miR-21, no band was observed. The miR-21 levels were able to be quantified using Quantity One. In Fig. 3B, the equation for the linear fit is relative intensity = −0.0371 + 0.0685 log(amol). The correlation coefficient of the data was 0.9942. The sensitivity is increased about 1000-fold after the silver enhancement. However, the 95% confidence intervals for each mean are large (Fig. 3B). It suggests that this method with silver enhancement can only be used for semi-quantification.

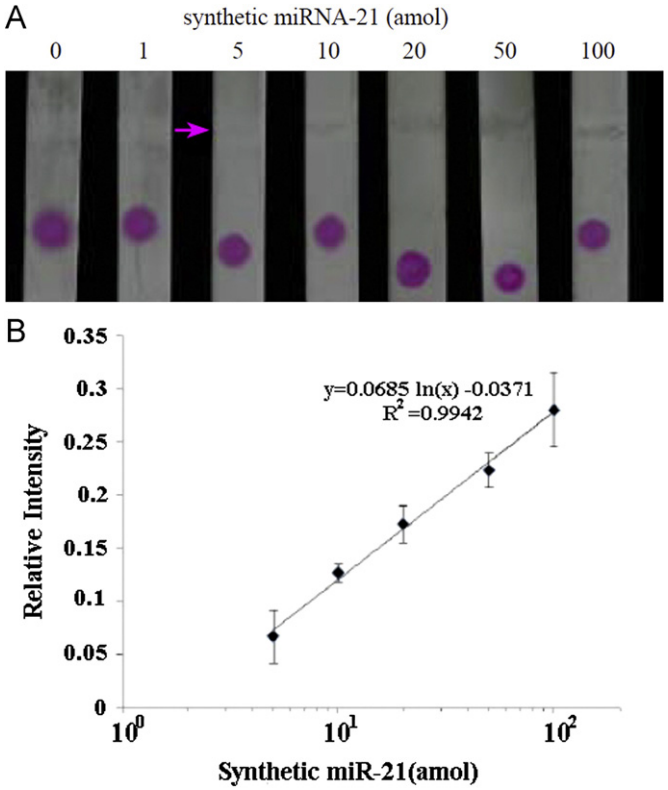

Fig. 3. Detection of miRNA-21 with silver enhancement. (A) Red band images for different levels of the miRNA-21 after silver enhancement. (B) Detection curve for miRNA-21. Each point represents the mean of six measurements from six separate experiments. The 95% confidence interval for each mean is between the error bars. The concentration of UDT, the blocking agent in this study, is 2.23 nM. The hybridization and mung-bean nuclease reaction time are 30 and 15 min, respectively. The reaction time for the silver enhancement is 15 min. The volume of DEPC-treated water containing tested miRNA is 100 μl. (For interpretation of the references to color in this figure legend, the reader is referred to the web version of this article.)

3.4. Optimization of UDT concentration for blocking AuNP-detection probe

After conjugation between the thiolated oligonucleotide detection probe and nanogold, UDT was used to block the naked surface of the gold nanoparticles. Without blocking, a band was observed in the negative control (data not shown). It is consistent with the results reported by He et al. [32]. However, we found that as the concentration of UDT increases, the intensity of the band decreases (Fig. 4). This suggests that the higher concentration of UDT replaces the thiolated oligonucleotide on the surface of the nanogold even if the colloidal gold was washed out of the UDT after one hour of the UDT treatment as described in the experimental section. Fig. 4 shows that in the negative control, no band was observed at the concentrations of 1.48, 2.23, and 4.46 nM. With silver enhancement, a faint band was observed at the concentration of 1.48 nM. These results suggest that avidin competing with BSA in the stop solution bound the naked surface of the gold nanoparticles if the concentration of UDT is not adequate to cover all the naked surface of the AuNPs. It resulted that the avidin–AuNPs bound the anti-avidin antibody in the test zone and the red bands were observed for negative control. At the concentration of 1.48 nM, no band was observed before silver staining because the amount of avidin–AuNPs is small. However, a faint band was observed after silver staining. Hence, the concentration of 2.23 nM was chosen as the assay condition for the data in Figs. 2 and 3.

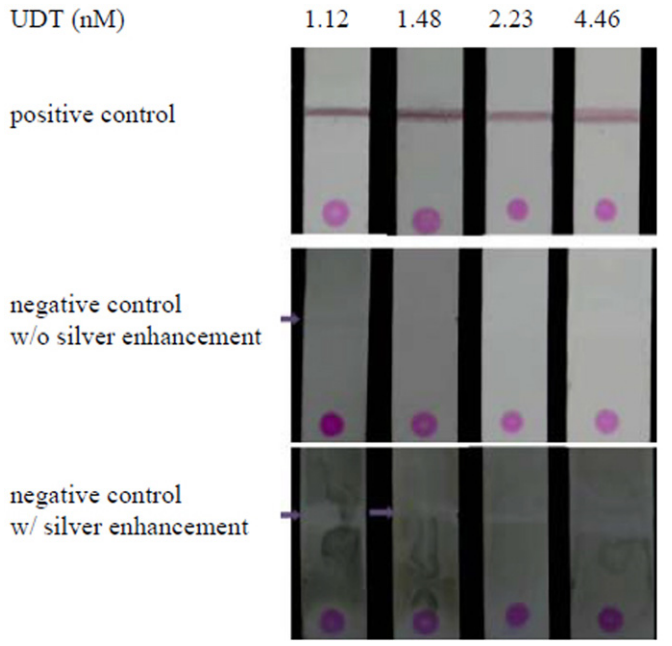

Fig. 4. Effects of the UDT concentrations. The image is the result from one of three separate experiments. The positive control contains detection probe–AuNP conjugates (0.18 nM) and 100 fmol of the biotin-bridge probe. The negative control contains the detection probe–AuNP conjugates (0.18 nM) and no biotin-bridge probe. Both controls were not treated by the mung-bean nuclease and the stop solution.

3.5. Optimization of hybridization time and reaction time

Fig. 5A shows the results for the different tested hybridization times. The relative density of the bands increased as the hybridization time increased. There was no significant difference in the relative intensity for assays between the hybridization time of 30 and 60 min. The hybridization time of 30 min was selected for all subsequent assays. The hybridization times of many other oligonucleotide assays are 30 or 60 min [31]. In a typical PCR experiment, the annealing time between oligonucleotide primers and a DNA template is 30 s which is much faster than the hybridization time in this assay. A possible reason is that the concentration of primers in the PCR, 10 μM, is much higher than the concentration of the capture probe in this assay, 2 nM. This suggests that researchers could increase the concentrations of the oligonucleotides in order to decrease the assay time. Fig. 5B shows the results for the different reaction times of the mung-bean nuclease. For the negative control, a faint band was observed after a 10 min treatment of the mung-bean nuclease, but no band was observed after a 15 min or longer treatment. For the positive control, the relative intensity of the band after 15 min treatment is stronger than after the 20 or 25 min treatment. Hence, the best reaction time for the mung-bean nuclease under the conditions we tested is 15 min.

4. Conclusion

It has been demonstrated here that the use of lateral flow nucleic acid test strips and gold nanoparticles can detect and quantify the miRNA level as low as 1 fmol and 5 amol without and with the silver enhancement, respectively. Unlike the traditional sandwich methods, the tested microRNA and the detection probe perfectly match the capture probe in this study. This design allows the miRNA to hybridize its capture probe at room temperature. It has been reported that it is necessary to block the

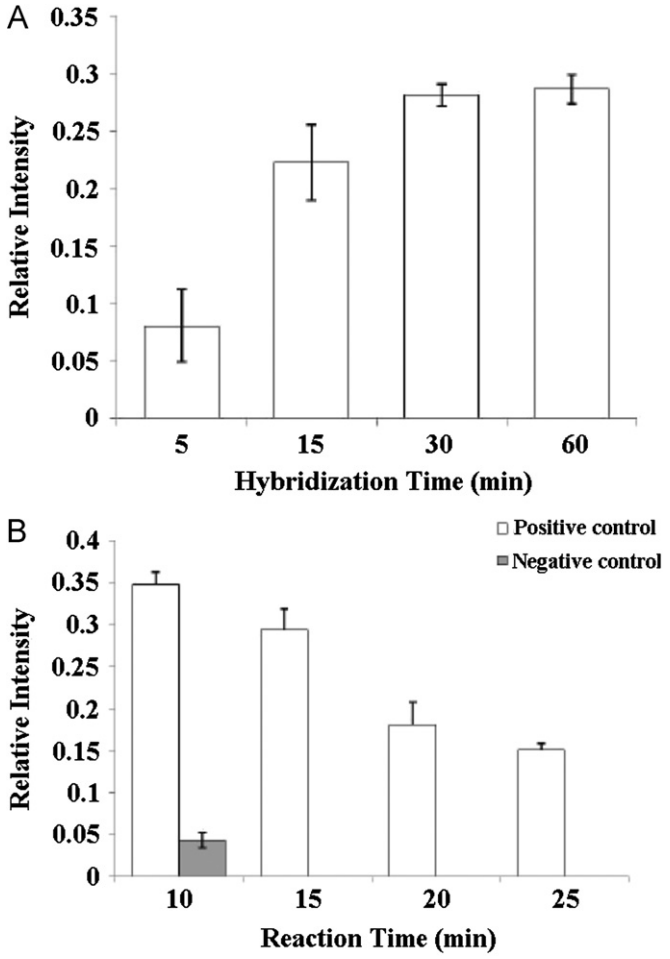

Fig. 5. Optimization of (A) hybridization time and (B) reaction time. Each column represents the mean of three measurements from three separate experiments. The 95% confidence interval for each mean is between the error bars. The concentration of UDT is 2.23 nM. The mung-bean nuclease reaction time is 15 min for the different hybridization times. The hybridization time is 30 min for the different reaction time.

naked area of AuNP even after the nanogold conjugates with the thiol-DNA [32]. Our data support this observation. Furthermore, we demonstrated here that the optimized concentration of a blocking agent, UDT in this study, exists. The entire procedure is very simple, and no expensive equipment is required. The assay takes about 70 min after the gold nanoparticle probe and sample preparations. Although we only reported that this assay could very effectively detect miRNA-21, this assay, in general, can be used for the detection of short oligonucleotides such as miRNA (21–25 nts) and siRNA (21–25 nts). The limitation of this methodology is that like northern blotting, it can only be used for semi-quantification because the 95% confidence intervals for each mean are large (Fig. 3).

References

[1] J.S. Mattick, I.V. Makunin, Hum. Mol. Genet. 14 (2005) R121–R132.
[2] D.H. Chitwood, M.C.P. Timmermans, Nature 467 (2010) 415–419.
[3] S. Davis, B. Lollo, S. Freier, C. Esau, Nucleic Acids Res. 34 (2006) 2294–2304.
[4] K.A. Cissell, S. Shrestha, S.K. Deo, Anal. Chem. 79 (2007) 4754–4761.
[5] Z. Gao, Z. Yang, Anal. Chem. 78 (2006) 1470–1477.
[6] S.H. Ramkissoon, L.A. Mainwaring, E.M. Sloand, N.S. Young, S. Kajigaya, Mol. Cell. Probe 20 (2006) 1–4.
[7] P.A. Maroney, S. Chamnongpol, F. Souret, T.W. Nilsen, RNA 13 (2007) 930–936.
[8] G.S. Pall, C. Codony-Servat, J. Byrne, L. Ritchie, A. Hamilton, Nucleic Acids Res. 35 (2007) e60.
[9] A. Válóczi, C. Hornyik, N. Varga, J. Burgyán, S. Kauppinen, Z. Havelda, Nucleic Acids Res. 32 (2004) e175.
[10] J. Li, B. Yao, H. Huang, Z. Wang, C. Sun, Y. Fan, Q. Chang, S. Li, X. Wang, J. Xi, Anal. Chem. 81 (2009) 5446–5451.
[11] H.-P. Yu, Y.-L. Hsiao, H.-Y. Pan, C.-H. Huang, S.-Y. Hou, Anal. Biochem. 419 (2011) 228–233.
[12] E. Lusi, M. Passamano, P. Guarascio, A. Scarpa, L. Schiavo, Anal. Chem. 81 (2009) 2819–2822.
[13] J. Li, B. Yao, H. Huang, Z. Wang, C. Sun, Y. Fan, Q. Chang, S. Li, X. Wang, J. Xi, Anal. Chem. 81 (2009) 5446–5451.
[14] X. Su, H.F. Teh, X. Lieu, Z. Gao, Anal. Chem. 79 (2007) 7192–7197.
[15] J.R. Mora, R.C. Getts, Biotechniques 41 (2006) 420.
[16] J. Lu, G. Getz, E.A. Miska, E. Alvarez-Saavedra, J. Lamb, D. Peck, A. Sweet-Cordero, B.L. Ebert, R.H. Mak, A.A. Ferrando, J.R. Downing, T. Jacks, H.R. Horvitz, T.R. Golub, Nature 435 (2005) 834–838.
[17] H.T. Allawi, J.E. Dahlberg, S. Olson, E. Lund, M. Olson, W.P. Ma, T. Takova, B.P. Neri, V.I. Lyamichev, RNA 10 (2004) 1153–1161.
[18] C.G. Liu, G.A. Calin, B. Meloon, N. Gamliel, C. Sevignani, M. Ferracin, C.D. Dumitru, M. Shimizu, S. Zupo, M. Dono, H. Alder, F. Bullrich, M. Negrini, C.M. Croce, Proc. Natl. Acad. Sci. USA 101 (2004) 9740–9744.
[19] S.-Y. Hou, H.-K. Chen, H.-C. Cheng, C.-Y. Huang, Anal. Chem. 79 (2007) 980–985.
[20] X. Mao, H. Xu, Q. Zeng, L. Zeng, G. Liu, Chem. Commun. 21 (2009) 3065–3067.
[21] Y. He, S. Zhang, X. Zhang, M. Baloda, A.S. Gurung, H. Xu, X. Zhang, G. Liu, Biosens. Bioelectron. 26 (2011) 2018–2024.
[22] X. Mao, Y. Ma, A. Zhang, L. Zhang, L. Zeng, G. Liu, Anal. Chem. 81 (2009) 1660–1668.
[23] B. Ngom, Y. Guo, X. Wang, D. Bi, Anal. Bioanal. Chem. 397 (2010) 1113–1135.
[24] K. Glynou, P.C. Ioannou, T.K. Christopoulos, V. Syriopoulou, Anal. Chem. 75 (2003) 4155–4160.
[25] I.K. Litos, P.C. Ioannou, T.K. Christopoulos, J. Traeger-Synodinos, E. Kanavakis, Anal. Chem. 79 (2007) 395–402.
[26] D.P. Kalogianni, T. Koraki, T.K. Christopoulos, P.C. Ioannou, Biosens. Bioelectron. 21 (2006) 1069–1076.
[27] M. Bendayan, Biotechnol. Histochem. 75 (2000) 203–242.
[28] W. Yang, X.-B. Li, G.-W. Liu, B.-B. Zhang, Y. Zhang, T. Kong, J.-J. Tang, D.-N. Li, Z. Wang, Biosens. Bioelectron. 26 (2011) 3710–3713.
[29] W.D. Kroeker, D. Kowalski, M. Laskowski, Biochemistry 15 (1976) 4463–4467.
[30] N. Desai, V. Shankar, FEMS Microbiol. Rev. 26 (2003) 457–491.
[31] Y.-T. Chen, C.-L. Hsu, S.-Y. Hou, Anal. Biochem. 375 (2008) 299–305.
[32] Y. He, K. Zeng, A.S. Gurung, M. Baloda, H. Xu, X. Zhang, G. Liu, Anal. Chem. 82 (2010) 7169–7177.